Oecologia
DOI 10.1007/s00442-014-2989-4

GLOBAL CHANGE ECOLOGY - ORIGINAL RESEARCH

Drought-induced increase in water-use efficiency reduces secondary tree growth and tracheid wall thickness in a Mediterranean conifer

José Miguel Olano · Juan Carlos Linares · Ana I. García-Cervigón · Alberto Arzac · Antonio Delgado · Vicente Rozas

Received: 4 March 2014 / Accepted: 29 May 2014

Abstract In order to understand the impact of drought and intrinsic water-use efficiency (iWUE) on tree growth, we evaluated the relative importance of direct and indirect effects of water availability on secondary growth and xylem anatomy of *Juniperus thurifera*, a Mediterranean anisohydric conifer. Dendrochronological techniques, quantitative xylem anatomy, and $^{13}C/^{12}C$ isotopic ratio were combined to develop standardized chronologies for iWUE, BAI (basal area increment), and anatomical variables on a 40-year-long annually resolved series for 20 trees. We tested the relationship between iWUE and secondary growth at short-term (annual) and long-term (decadal) temporal scales to evaluate whether gains in iWUE may lead to increases in secondary growth. We obtained a positive long-term correlation between iWUE and BAI, simultaneously with a negative short-term correlation between them. Furthermore, BAI and iWUE were correlated with anatomical traits related to carbon sink or storage (tracheid wall thickness and ray parenchyma amount), but no significant correlation with conductive traits (tracheid lumen) was found. Water availability during the growing season significantly modulated tree growth at the xylem level, where growth rates and wood anatomical traits were affected by June precipitation. Our results are consistent with a drought-induced limitation of tree growth response to rising CO_2, despite the trend of rising iWUE being maintained. We also remark the usefulness of exploring this relationship at different temporal scales to fully understand the actual links between iWUE and secondary growth dynamics.

Keywords Basal area increment (BAI) · Intrinsic water-use efficiency (iWUE) · *Juniperus thurifera* · Mediterranean climate · Xylem quantitative anatomy

Introduction

CO_2 concentration in the atmosphere has risen to approximately 30 % above preindustrial concentrations and is likely to continue rising in the near future (IPCC 2013). Increased atmospheric CO_2 concentrations have a direct

Communicated by David Tissue.

Electronic supplementary material The online version of this article (doi:10.1007/s00442-014-2989-4) contains supplementary material, which is available to authorized users.

J. M. Olano (✉) · A. I. García-Cervigón
Departamento de Ciencias Agroforestales, EU de Ingenierías Agrarias, Universidad de Valladolid, Los Pajaritos s/n, 42004 Soria, Spain
e-mail: jmolano@agro.uva.es

J. M. Olano · A. I. García-Cervigón
Sustainable Forest Management Research Institute, Universidad de Valladolid-INIA, Valladolid, Spain

J. C. Linares
Área de Ecología, Universidad Pablo de Olavide, Ctra. Utrera km. 1, 41002 Seville, Spain

A. Arzac
Departamento de Biología Vegetal y Ecología, Facultad de Ciencia y Tecnología, Universidad del País Vasco, Barrio Sarriena s/n, 48940 Leioa, Bizkaia, Spain

A. Delgado
Instituto Andaluz de Ciencias de la Tierra (CSIC), 18100 Armilla, Granada, Spain

V. Rozas
Laboratorio de Dendrocronología, Facultad de Ciencias Forestales, Universidad Austral de Chile, Casilla 567, Valdivia, Chile

Published online: 24 June 2014

effect on plant growth (Körner 2000), as CO_2 is the source of carbon for photosynthesis. Higher CO_2 levels therefore enhance photosynthetic rates and the ratio of C assimilated to water transpired, i.e. the intrinsic plant water-use efficiency (iWUE; McCarroll and Loader 2004). In addition, CO_2 is the most important long-lived greenhouse gas related to current global warming. An increase in atmospheric CO_2 thus also affects plant carbon uptake indirectly, through its impact on global climate (IPCC 2013). An understanding of the direct and indirect effects of atmospheric CO_2 concentrations on tree growth is critical in order to predict ecosystem responses to ongoing, and expected, CO_2 and temperature rises (Körner 2000).

A positive effect of rising CO_2 on plant iWUE, photosynthetic rate, and growth has been described (Norby et al. 2010; Dawes et al. 2013). Accordingly, worldwide increasing iWUE reports have been described during the past century (Saurer et al. 2004; Peñuelas et al. 2011), although the rate of increase is extremely variable and there is a trend to reach a saturation-like asymptote (Waterhouse et al. 2004; Peñuelas et al. 2011). However, this increase in iWUE is not clearly related to increasing tree growth rates. In fact, tree growth has declined in some species, despite increases in iWUE (Saurer et al. 2004; Peñuelas et al. 2011). Different factors have been proposed to explain why increases in iWUE may not be linked to higher growth rates: rising temperatures (Linares and Camarero 2011), increasing drought frequency and severity (Barber et al. 2000; Heres et al. 2013), herbivore effects (Speed et al. 2011), nutrient limitation (Körner 2000), higher competition levels (Linares et al. 2009), and physiological adaptations (Waterhouse et al. 2004).

Direct and indirect effects of atmospheric CO_2 are especially relevant on Mediterranean-type ecosystems, where tree species show a strong year-to-year growth and iWUE variability (Maseyk et al. 2011). This annual variation has been usually attributed to climatic constraints, mainly drought, on carbon assimilation (Ferrio and Voltas 2005). Notwithstanding, summer drought is one of the major forces limiting tree growth, with its effects operating at multiple functional and temporal scales (Pasho et al. 2011). Some results suggest that year-to-year variability in iWUE and tree growth may be responding to similar climatic constraints leading to a correlation between both parameters (Andreu et al. 2008; Maseyk et al. 2011). Therefore, disentangling the effect of climate on iWUE and secondary growth is crucial to understanding plant response to a drier climate. Focusing on the analysis of year-to-year variability has been successful to isolate climate effect from other co-occurring factors because it removes low to mid-temporal collinearity with other potentially confounding factors such as tree age (Bert et al. 1997), competition (Linares et al. 2009), or changes in nutrient levels (Koehler et al. 2012). This approach may provide information about how climate, iWUE, and secondary growth interact at yearly scales, and contribute to a better understanding of this high-frequency signal in long-standing (decadal) trends between iWUE and growth.

Xylem structure records life-time information on anatomical adjustments to environmental conditions (Fonti et al. 2010). The use of the high-frequency (annual) signal in anatomical information may allow a better interpretation of the functional dependence of secondary growth on iWUE. If the effect of iWUE is mediated by changes in carbon availability (Galiano et al. 2011; Kilpeläinen et al. 2007), we would expect that the patterns of carbon gain reflected in iWUE would impact xylem characteristics associated to carbon sink and storage, particularly cell wall thickness and the amount of parenchyma. Moreover, understanding the combined influence of iWUE and secondary growth on wood structure is desirable as anatomical variations may modulate xylem functional properties (Hacke and Sperry 2001; Fonti et al. 2010), and minor changes in anatomical traits may affect the ability of trees to cope with constraints associated with environmental change.

Our aim was to evaluate the relative importance of direct and indirect (mediated by iWUE) effects of water availability on secondary growth and carbon allocation of *Juniperus thurifera* L., a long-lived anisohydric conifer inhabiting continental Mediterranean climate, where the growing season is constrained by drought (Camarero et al. 2010). We compiled a detailed dataset comprising annually resolved data for iWUE, secondary growth, and wood anatomy (lumen diameter, wall thickness, and proportion of parenchyma) for 20 trees over a 40-year period. We used structural equation modeling (SEM) to analyze our data, since SEM allows the assessment of simultaneous direct and indirect causal effects among a given set of interrelated variables (Grace 2006). Finally, we compared the relationship between iWUE and secondary growth at short-term (annual) and long-term (decadal) temporal scales to evaluate whether gains in iWUE may lead to increases in secondary growth (Granda et al. 2014).

Materials and methods

Study species

Juniperus thurifera (Spanish juniper) is a long-lived evergreen tree endemic to the western Mediterranean basin. In our study area (see below), radial growth of this species responds negatively to winter precipitation and positively to summer precipitation (Rozas et al. 2009; DeSoto et al. 2012; Granda et al. 2013). Xylogenesis starts in early May and ends in late October, with latewood comprising

a small part of the ring (<4 %) and being formed in a distinct period starting in early August (Camarero et al. 2010). Water availability during summer (June–July) is the main factor determining earlywood lumen size and wall thickness (Olano et al. 2012), whereas ray parenchyma abundance mainly responds positively to May precipitation (Olano et al. 2013b). Photosynthetic activity is maintained all year round, and reaching a maximum during spring (Gimeno et al. 2012).

Study area

The study area is a 3,300-ha woodland located at Sierra de Cabrejas, 30 km west of Soria city, in northcentral Spain (41°46′N, 02°49′W; 1,100–1,300 m a.s.l.). Parent rock is Cretaceous limestone, and soils are calcium-rich and shallow. *Juniperus thurifera* forms an open woodland with a mean density of over 300 trees ha^{-1}, coexisting with pines (*Pinus sylvestris* L. and *P. pinaster* Ait.) and Holm oak (*Quercus ilex* L.). Climate is subhumid, continental Mediterranean. Records of mean monthly temperature and total monthly precipitation were obtained from the Soria meteorological station (41°46′N, 02°28′W; 1,082 m altitude, 30 km away from the study site) for the period 1965–2004. Annual mean temperature is 10.4 °C, the coldest month being January (mean daily minimum temperature of −1.8 °C) and the warmest July (mean daily maximum temperature of 28.1 °C). Average annual precipitation is 556 mm, with a summer drought period typically occurring between July and August (Fig. 1a). Drought, considered as precipitation amount in millimeters being lower than twice the temperature value in Celsius, occurs in June in 50 % of years, and in July and August in over 70 % of years (Fig. 1b).

Sampling design

One stem disc at 1.3 m above ground was taken from each of the 20 trees that had been felled during the winter of 2004–2005, based on a regular sampling design (for details, see Olano et al. 2008). These stem discs were mechanically surfaced and then manually polished with a series of successively finer grades of sandpaper until the xylem cellular structure was clearly visible under a magnifying lens. On each disc, two radii were selected along sectors with more regular tree-ring growth, and tree-ring sequences along these radii were dated with the help of a robust chronology available for the same study site (Rozas et al. 2009). Total ring widths were measured to the nearest 0.001 mm with a Velmex sliding-stage micrometer (Velmex Inc., Bloomfield, NY, USA) interfaced with a computer. The software COFECHA (Grissino-Mayer 2001) was used to check the crossdating. As age and sex affect the response

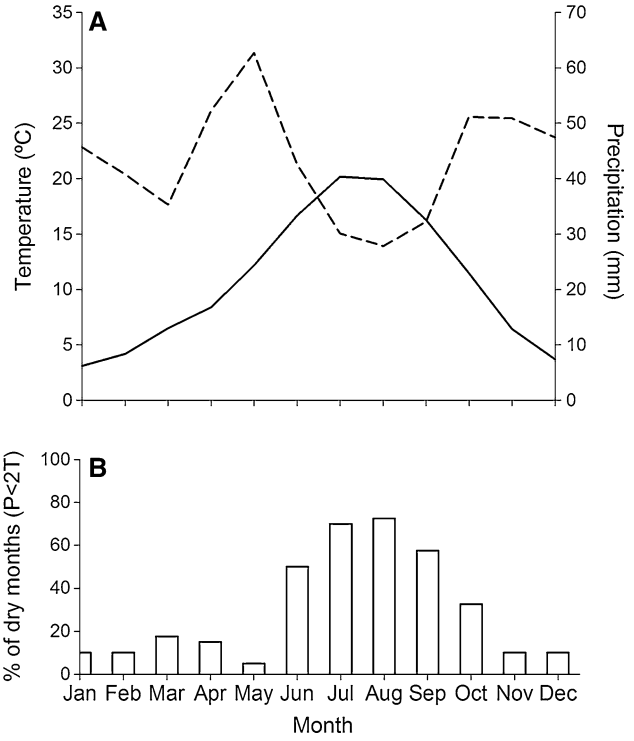

Fig. 1 **a** Climatic diagram from Soria meteorological station for the period 1965–2010. The *dashed line* represents monthly accumulated precipitation and the *continuous line* indicates mean monthly temperature. **b** Percentage of dry months (P < 2T) for the period 1965–2004

of *J. thurifera* to climate (Rozas et al. 2009), we chose ten young (<150 year) and ten old (>150 year) trees, and a similar, but not identical, number of male and female trees per age class (six males and four females for young trees, five per sex for old trees) to get a representative sampling of the species response, avoiding any potential age- or sex-related effect derived from skewed sampling. Basal area increment (BAI) was used as a surrogate of secondary growth, as it is a more biologically meaningful descriptor of growth trends than ring widths (Biondi and Qeadan 2008). BAI was calculated using the formula

$$\mathrm{BAI} = \pi \left(r_t^2 - r_{t-1}^2 \right) \quad (1)$$

where r is the tree radius and t is the year of tree-ring formation.

Anatomical parameters

A 5-mm-wide and approximately 1.5-cm-thick piece was cut out from every disc along the best crossdated radius. This piece was cut longitudinally in two halves to obtain two replicates. One half was used for anatomical analysis and another half was used for stable carbon isotope ratio analysis. Cross sections thinner than 15 µm were cut with a

sledge microtome (H. Gärtner/F. H. Schweingruber, WSL, Birmensdorf, Switzerland) and then placed on a slide and stained with Alcian blue (Alcian blue 1 % solution in acetic acid) and Safranin (Safranin 1 % solution in ethanol), which resulted in unlignified cells appearing blue and lignified cells appearing red. Afterwards, the thin-sections were dehydrated using a series of solutions of increasing ethanol concentration, washed with xylol, and then permanently preserved by embedding them into Eukitt glue (Kindler GmbH, Freiburg, Germany). Images of each annual ring were captured with a Nikon D90 digital camera mounted on a Nikon Eclipse 50i optical microscope with 200× magnification. When an annual ring could not be captured in a single photograph, sequential images were merged (PTGUI, ver. 8.3.10 pro, New House Internet Services B.V., Rotterdam, The Netherlands). Image analysis was performed with ImageJ (v. 1.44; http://rsb.info.nih.gov/ij; W. Rasband, National Institutes of Health, Bethesda, MD, USA).

Cell dimensions, including lumen radial diameter and radial cell wall thickness, were measured for each tracheid along three radii per annual ring for a 40-year period (1965–2004). Individual cells were assigned to earlywood or latewood portions according to Mork's index (Denne 1988). Measurements for cell dimensions were normalized to standard numbers of cells (three for earlywood and one for latewood) with the tgram package (DeSoto et al. 2011) in R (R Development Core Team 2011). See more detailed information on this procedure in (Olano et al. 2012). Percentage of parenchyma in wood rays was estimated as the quotient between the area occupied by ray parenchyma and the total ring area analyzed, according to the detailed procedure explained in (Olano et al. 2013b). As a result, we obtained eight annually resolved chronologies for each individual: number of xylem tracheids (NTra), three estimates of lumen diameter (LUM1, LUM2, LUM3), and three of wall thickness (Wall1, Wall2, Wall3), corresponding to each third of earlywood, and lastly the percentage of ray parenchyma (PERPAR). Latewood was not considered for this analysis as its contribution to final ring width is negligible (<4 %).

Estimation of water-use efficiency

To assess annual changes in water-use efficiency of individual trees, we evaluated their $^{13}C/^{12}C$ isotope ratios ($\delta^{13}C$) in wood from cross-dated annual tree rings from the period 1965–2004 when atmospheric CO_2 levels rose from 322.13 to 380.41 ppm (data from Mauna Loa Observatory, Hawaii). Earlywood from each of the annual rings of each tree was separated with a scalpel under a binocular lens and homogenized using a mill (Culatti MFC). Cellulose was not extracted as several studies show good correlations between $\delta^{13}C$ in wood and cellulose, even at the intra-seasonal level, and therefore both show similar relationships related to atmospheric CO_2 and climate (Taylor et al. 2008; Roden and Farquhar 2012). The wood powder was weighed into tin cups and combusted to CO_2 in an elemental analyzer attached to an isotope-ratio mass spectrometer (Thermo Finnigan MAT 251). Results were expressed as relative differences in $^{13}C/^{12}C$ ratio of tree-ring wood in parts per thousand (‰) relative to the standard V-PDB ($\delta^{13}C_{plant}$). $\delta^{13}C_{plant}$ was used to calculate isotopic discrimination (Δ; Farquhar and Richards 1984). We then calculated the intrinsic water-use efficiency (iWUE; expressed in μmol of CO_2 per mol of H_2O), using available data of $\delta^{13}C$ in atmospheric CO_2 and atmospheric CO_2 concentrations (see McCarroll and Loader 2004 for a detailed description of iWUE calculation).

Computation of standardized chronologies

In order to obtain robust chronologies of yearly variation for the 20 raw individual time series, we standardized the ten variables (iWUE, BAI, NTra, PERPAR, LUM1, LUM2, LUM3, Wall1, Wall2, and Wall3) using the ARSTAN program (Cook and Holmes 1996). This program accomplishes a time series treatment to remove trends in the values as well as different levels of temporal autoregression, leading to stationary and free from temporal autocorrelation time series of the analyzed parameters. Trend was removed following a two-step procedure; the series were first fitted to a negative exponential or straight line, and then to a cubic smoothing spline with a 50 % frequency response of 20 years, which is flexible enough to reduce considerably non-climatic variance (Helama et al. 2004). Individual series for each of the 20 trees were combined using a biweight robust mean to obtain a chronology for each measured variable.

Structural equation modeling

Structural equation models (SEM) were used to evaluate simultaneously the interrelations between climate, water-use efficiency, secondary growth, and wood anatomy. These models assess how well data support a set of hypothesized causal relationships between different variables by including both direct and indirect effects (Grace 2006). The number of variables to be included in the model was constrained by sample size ($n = 40$ years), therefore we had to reduce our set of variables. BAI and iWUE were included, as well as June precipitation as a measure of water availability during the growing season (see Fig. S1 for the climate-growth relationships of the studied chronologies). Alternative measurements to June precipitation, such as accumulated May–July precipitation, evapotranspiration

rates, or standardized precipitation evapotranspiration indices (Vicente-Serrano et al. 2010) were explored, but although they may be slightly higher correlated to some individual variables, they did not improve the global explanation of the studied variables. To detect collinearities among anatomical variables, we used a correlation matrix among the ten standardized chronologies. Highly correlated variables may cause problems when estimating path coefficients (Grace 2006), so we excluded NTra because it was redundant with BAI. Measurements of lumen diameter were also excluded because they did not show a relationship to iWUE, BAI, or to any other anatomical variables.

Model specification

Based on existing knowledge, we hypothesized that water availability during the growing season (June precipitation) would exert an effect on iWUE, BAI, and on the first two-thirds of earlywood cell walls that matured during that period (paths from P June to iWUE, BAI, Wall1 and Wall2; Camarero et al. 2010; Olano et al. 2012). It is important to remark that carbon acquisition is previous to xylem formation and thus relations from iWUE to anatomical characteristics and secondary growth are expected to be unidirectional. The independence between growth-year lumen diameters and iWUE supported that variations in iWUE were expected to reflect carbohydrate gains (Galiano et al. 2011), thus leading to changes in the different carbon sinks (paths from iWUE to BAI, PERPAR, Wall1, Wall2, and Wall3). Larger BAI means a larger conductive area, mainly due to an increase in the number of tracheids, thus probably leading to an increase in carbon gain and more available resources to increase wall thickness (Ponton et al. 2001). In our study area, tracheid expansion occurs mostly during May and June, but tracheids are not functional until the end of the maturation phase that may occur much later in the season, from mid June to late July (Camarero et al. 2010). Any potential effect of increase of conductive area (larger BAI) in resource acquisition would only be apparent at the end of the growing season in late June and July, thus restricting its potential effects to processes occurring after that period, namely wall thickening of the second (Wall2) and specially the third (Wall3) thirds of the earlywood tracheids. An effect of wall thickness on BAI is not probable because tracheid thickening occurs after cell expansion, without a direct impact on final tracheid size. Carbon stored in ray parenchyma (PERPAR) may be remobilized during the growing season and invested in other carbon sinks, leading to paths from PERPAR to BAI, Wall1, Wall2, and Wall3. Finally, tracheid wall thickness was expected to show a strong temporal covariation between different segments of the ring (double-headed arrows between Wall1, Wall2, and Wall3), due to a common response to the environmental constraints that control wall formation.

Endogenous variables met multinormality, and estimation of model parameters was based on maximum likelihood. The validity of the model was tested by the goodness-of-fit index (GFI) and root mean square error of approximation (RMSEA). GFI is independent of the estimation method and ranges between 0 and 1, with values above 0.90 indicating a good fit (Grace 2006). RMSEA is based on predicted versus observed covariance, as a result of it being less affected by sample size, and includes a correction for model complexity. RMSEA is less than 0.05 for very good models (those with a close fit), less than 0.1 for models that fit adequately, and greater than 0.1 for poorly fitted models. Analyses were conducted with AMOS 18.0 (Arbuckle 2009).

Finally, in order to assess whether the relationship between secondary growth and iWUE differed at contrasting frequency domains, we correlated BAI with iWUE raw values (mid to low frequency domain, decadal trends) and BAI with iWUE standardized chronologies (high-frequency domain, yearly variation).

Results

Tree age was 84 ± 32 years (mean ± SD) for young trees and 224 ± 45 years for old trees. The studied trees showed low growth rates during the study period, with tracheid lumen diameters decreasing along the tree ring (Table 1). Radial wall thickness, however, was rather uniform along the earlywood, ranging from a maximum of 3.58 ± 0.59 (mean ± SE) μm in the mid part of the earlywood to a minimum of 3.46 ± 0.60 μm in the final part (Table 1). Mean correlation between trees (r_{bt}) was very high for iWUE, very low for PERPAR, and intermediate for the rest of the variables (Table 1). First-order autocorrelation values (AC1) were low for iWUE and Wall2, and very low for the other variables. Expressed population signal (EPS) was very high for iWUE, high for BAI and NTra, and moderate for the other variables, with the exception of PERPAR that had a very low value.

Highly significant negative correlations of iWUE with BAI, Wall2, and Wall3 were found, marginally significant with PERPAR and LUM2 (Table 2). BAI and NTra showed a very strong correlation ($r = 0.937$, $p < 0.001$), indicating that annual variability in BAI respond largely to variation in the number of tracheids, both parameters being redundant. BAI also showed a positive correlation with PERPAR, Wall2, and Wall3. PERPAR was positively correlated with Wall2 and Wall3, and wall thickness values were also inter-correlated in the different portions of the annual ring. Lumen diameters showed significant correlations

Table 1 Summary statistics for standardized chronologies based on 20 *Juniperus thurifera* individuals in the common period 1965–2004

Parameter (units)	Acronym	Mean ± SD	r_{bt}	AC1	EPS
Basal area increment (mm^2 $year^{-1}$)	BAI	407 ± 381	0.241	−0.082	0.870
Number of tracheids	NTra	39.30 ± 0.71	0.286	−0.027	0.884
Intrinsic water-use efficiency (μmol C mol H_2O^{-1})	iWUE	112 ± 11	0.784	0.151	0.986
Ray parenchyma area (%)	PERPAR	6.67 ± 1.89	−0.002	−0.047	−0.038
1st Earlywood third radial wall thickness (μm)	Wall1	3.55 ± 0.58	0.070	0.078	0.600
2nd Earlywood third radial wall thickness (μm)	Wall2	3.58 ± 0.59	0.070	0.125	0.600
3rd Earlywood third radial wall thickness (μm)	Wall3	3.46 ± 0.60	0.115	−0.031	0.722
1st Earlywood third radial lumen diameter (μm)	LUM1	16.23 ± 3.08	0.085	0.057	0.666
2nd Earlywood third radial lumen diameter (μm)	LUM2	14.71 ± 2.80	0.128	0.034	0.746
3rd Earlywood third radial lumen diameter (μm)	LUM3	11.73 ± 4.51	0.057	0.014	0.508

r_{bt} Mean correlation between trees, *AC1* first-order autocorrelation, *EPS* expressed population signal

Table 2 Pairwise Pearson's correlations between the ten standardized *Juniperus thurifera* chronologies

	BAI	NTra	iWUE	PERPAR	WALL1	WALL2	WALL3	LUM1	LUM2
NTra	**0.937**	–	–	–	–	–	–	–	–
iWUE	**−0.577**	**−0.529**	–	–	–	–	–	–	–
PERPAR	*0.344*	0.249	**−**0.300	–	–	–	–	–	–
Wall1	0.225	0.256	−0.174	0.275	–	–	–	–	–
Wall2	**0.605**	**0.613**	**−0.573**	**0.566**	**0.498**	–	–	–	–
Wall3	**0.537**	**0.563**	−0.468	*0.368*	*0.349*	**0.574**	–	–	–
LUM1	0.082	0.016	−0.195	0.001	−0.137	0.002	0.051	–	–
LUM2	0.274	0.108	−0.302	0.032	−0.093	−0.151	−0.024	**0.748**	–
LUM3	0.069	−0.085	−0.107	−0.066	−0.124	−0.140	0.209	**0.531**	**0.678**

Coefficients in *bold* are significant at $p < 0.001$, *underlined* at $p < 0.01$, and in *italic* at $p < 0.05$

Table 3 Path coefficients of total, direct, and indirect effects of variables used in the SEM

	P June			iWUE			BAI			PERPAR		
	Total	Direct	Indirect	Total	Direct	Indirect	Total	Direct	Indirect	Total	Direct	Indirect
iWUE	−0.349	**−0.349**	0.000	–	–	–	–	–	–	–	–	–
BAI	0.482	**0.319**	0.162	−0.464	**−0.403**	−0.061	–	–	–	0.202	0.202	0.000
PERPAR	0.105	0.000	0.105	−0.300	**−0.300**	0.000	–	–	–	–	–	–
Wall1	0.395	**0.381**	0.014	−0.040	0.039	−0.079	–	–	–	0.262	**0.262**	0.000
Wall2	0.336	0.059	0.277	−0.516	**−0.262**	−0.253	0.302	**0.302**	0.000	0.438	**0.377**	0.061
Wall3	0.265	0.000	0.265	−0.426	−0.203	−0.223	0.362	**0.362**	0.000	0.255	0.181	0.073

Direct effects are path coefficients shown in Fig. 2. Note that total is the sum of direct and indirect effects. In *bold* are direct path effects significant at $p < 0.05$

between them, but were independent of any other variable considered.

SEM provided an excellent overall fit for our data set (Fig. 2). The significance of χ^2 estimate was greater than 0.05 ($df = 3$, $\chi^2 = 0.181$, $p = 0.981$), with GFI being greater than 0.90 (0.999) and RMSEA being lower than 0.1 (0.000). The percentage of variance explained by the model was large for BAI (46 %), Wall2 (57 %), and Wall3 (36 %). The model revealed a simultaneous presence of direct paths from June precipitation to iWUE, BAI, and Wall1, but not on Wall2. iWUE had significant negative paths on BAI, PERPAR, and Wall2. BAI had significant positive paths on Wall2 and Wall3. PERPAR had a significant positive path on Wall2 and an only marginally significant path on Wall1. Only the covariance between Wall1 and Wall2 was significant. June precipitation also exhibited indirect effects on all endogenous variables except iWUE (Table 3), remarkably on Wall2 and Wall3, mediated by iWUE, BAI, and PERPAR, and on BAI mediated by iWUE. iWUE had a strong negative indirect effect on Wall2 and Wall3 mediated by BAI and PERPAR.

BAI and iWUE raw values showed an increasing trend along the study period (Fig. 3a), and were highly positively correlated ($r = 0.537$, $p < 0.001$). BAI and iWUE

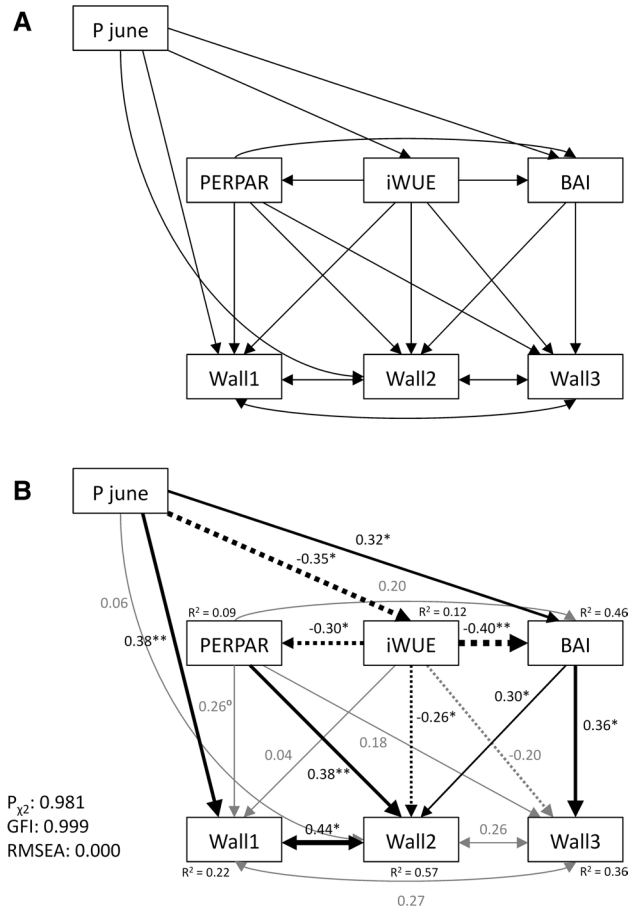

Fig. 2 Hypothetical structural equation model (**a**) for climate (P June), intrinsic water-use efficiency (iWUE), basal area increment (BAI), and xylem anatomy (percentage of ray parenchyma—PERPAR—and wall thickness—Wall1, Wall2, Wall3) and fitted model to the data (**b**). *Single-headed arrows* indicate causal relationships, and *double-headed arrows* indicate covariation. *Numbers* in paths indicate standardized regression weights. Positive effects are indicated by *solid lines* and negative effects by *dashed lines*. *Arrow widths* are proportional to path coefficients. R^2 explained variance for each endogenous parameter. $*p < 0.05$, $**p < 0.01$

standardized indices (Fig. 3b), on the other hand, showed a strong negative correlation ($r = -0.577$, $p < 0.001$). These results suggest that, while the long-term trend was similar between both parameters, the high-frequency inter-annual variation of BAI and iWUE showed the opposite pattern.

Discussion

SEM analysis allowed to disentangle complex annual interactions between climate, iWUE, secondary growth dynamics, and wood anatomical characteristics in the Mediterranean tree *J. thurifera*. Water availability during the growing season affected BAI, iWUE, and several anatomical variables. Annual variation of iWUE showed a strong negative correlation with BAI that remained even after controlling the effect of their common response to June precipitation. Yearly variation in secondary growth and iWUE was strongly related to xylem anatomical variables related to carbon sink or storage, pointing to an effect of iWUE on xylem anatomy mediated by changes in carbohydrates availability (Galiano et al. 2011; Kilpeläinen et al. 2007).

Water availability regulates gas exchange at the leaf level, with dry conditions usually leading to more water-efficient stomatal behavior (Ferrio and Voltas 2005; Andreu et al. 2008). On the other hand, higher water availability during the growing season may exert a positive effect on the role of xylem as a carbon sink through increased cambial cell division rates (Camarero et al. 2010), higher cell expansion (Von Wilpert 1991), longer wall maturation times (Cuny et al. 2013), and a longer growing season (Eilmann et al. 2011). Our results support that water availability exerts a (partially) independent effect on these parameters as pointed out by the maintenance of direct paths from June precipitation to iWUE, Wall1, and BAI, with BAI closely related to the total tracheid number in the tree ring.

A negative relationship between the high-frequency (yearly) variation of iWUE and secondary growth has already been reported in the literature (Andreu et al. 2008; Maseyk et al. 2011). Even if a significant amount of C-acquisition might occur prior to ring formation, the influence of iWUE on BAI included the synergistic effect of an iWUE-mediated impact of June precipitation on BAI, and a direct effect on iWUE that was independent of June precipitation. This is supported by the lower value of the path coefficient between June precipitation and BAI compared with the correlation coefficient (0.31 versus 0.47). Drought induces stomatal closure and decreases photosynthetic rates even in anisohydric species such as *J. thurifera* (McDowell 2011), suggesting that high-frequency improvements in iWUE may be linked to reductions in stomatal conductance to water vapor, hence reducing water loss, rather than to higher photosynthetic rates (Linares and Camarero 2011). Thus, the negative relationships between high-frequency iWUE and BAI variation could be interpreted as a direct impact of reduced carbon assimilation on secondary growth, as was also recently shown by (Galiano et al. 2011). This result would be supported by the negative impact of iWUE on other carbon sinks, such as ray parenchyma abundance and tracheids' wall thickness (Wall2). Interestingly, iWUE did not show any significant correlation with lumen diameters, thus reinforcing our hypothesis of a carbon-mediated impact of iWUE on xylem anatomy. However, it should be also taken into account that we estimated iWUE values (i.e., a leaf-level process) from wood $\delta^{13}C$, while fractionations from leaf to trunk could also affect wood carbon isotope signal (Helle and Schleser 2004; Offermann et al. 2011).

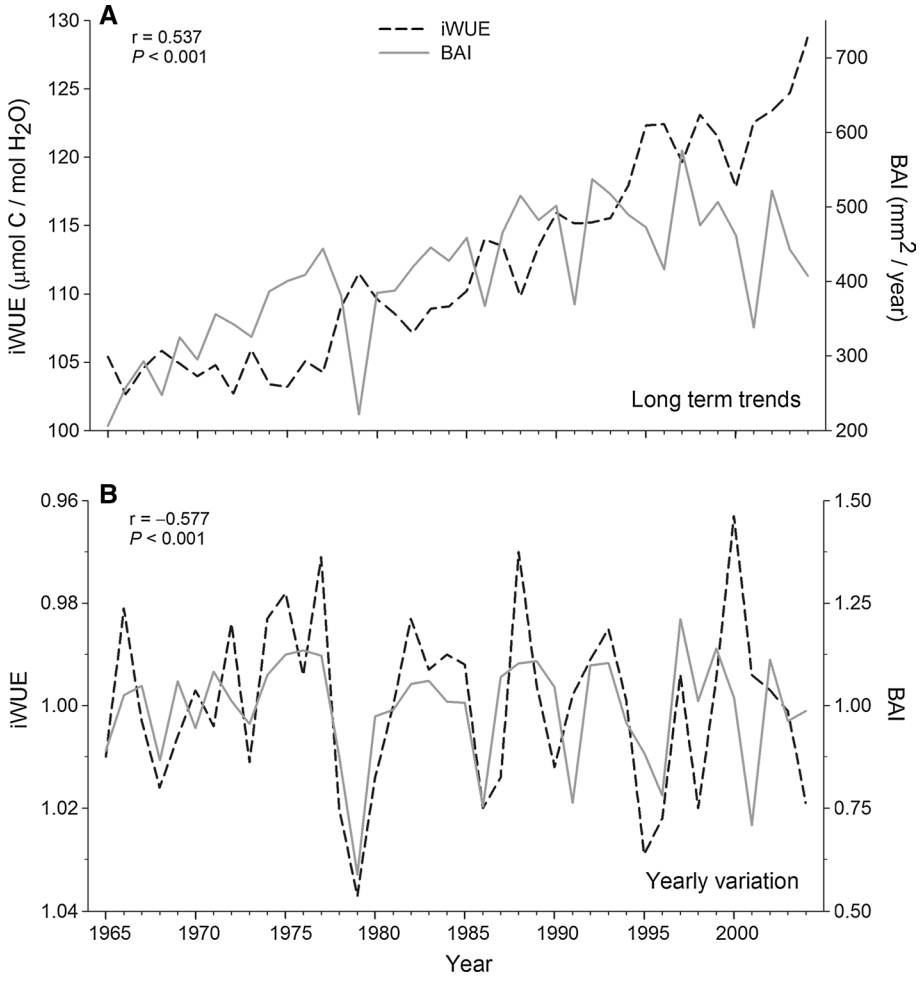

Fig. 3 Relationships between intrinsic water-use efficiency (iWUE) and basal area increment (BAI). **a** Long-term trends based in raw values and **b** yearly variation based in standardized chronologies. Data are based on 20 *Juniperus thurifera* trees for the period 1965–2004. Note that iWUE axis is inverted in **b**

Carbon allocation to different xylem structures and functions is subjected to trade-offs that regulate the differential investment among cellular elements (Chave et al. 2009), which may lead to negative correlations among them, for example denser xylem versus larger growth rate. In our case, these trade-offs did not occur, as was shown by the strong positive correlations between BAI, PERPAR, and radial wall thickness. During favorable years, junipers built wider rings showing numerous tracheids with thicker walls and abundant storage tissue. This pattern agrees with the observed response of drought-stressed *P. sylvestris* in an experimental study, in which irrigation led to wider annual rings and thicker tracheid walls (Eilmann et al. 2010, 2011). This would suggest that constraints for resource allocation among carbon sinks and reservoirs were overridden in importance by the inter-annual variation in water availability and photosynthetic rates. This means either that under favorable conditions more carbon is supplied to all xylem compartments, or that there is no internal competition, but rather coordination, among carbon sinks. This second hypothesis would imply that the different sinks are prevented from carbohydrates deprivation as long as there are sufficient resources. The negative impact of water-use efficiency on radial wall thickness suggests that when drought induces an increase in iWUE, the role of xylem as a carbon sink may be minimized, with an associated reduction in secondary growth rate.

The maintenance of direct significant relationships between secondary growth rates and wall thickness, even after controlling for the effect of June precipitation, suggests that additional functional mechanisms, not directly related to climate, may promote these positive interactions. The influence of BAI on tracheid wall thickness varied along the annual ring, with no effect in the first third of earlywood, and a strong effect in the last third. This is congruent with our hypothesis that a larger BAI implies more tracheids and higher conductive area in conifers, and this positive effect would only occur after tracheid maturation, being only remarkable for the final parts of the ring. Larger xylem conductivity increases resource acquisition, triggering higher carbon investment in secondary growth and higher growth rates (Tyree 2003; Ze-Xin et al. 2012; Olano et al. 2013a). The robust path between BAI and Wall3 diminishes the chance of results being influenced

by confounding climatic effects. Remarkably, this effect is maintained even when July climatic conditions are considered (data not shown). However, the strong positive correlation between BAI and iWUE raw values was coupled to a significant negative correlation between their high-frequency inter-annual variations, as previously found for other drought-constrained conifers (Rathgeber et al. 2011). Furthermore, the positive effect of PERPAR on wall thickness might be interpreted as a consequence of the remobilization of carbohydrates stored in ray parenchyma later in the growing season in order to contribute to current xylem maturation. The decrease of this effect in the late earlywood might correspond to a more prominent role of the carbohydrates stored in the parenchyma in maintaining water conductive safety during the summer drought (Salleo et al. 2009).

Decadal trends of iWUE and secondary growth are congruent with the highly positive response of *J. thurifera* secondary growth to increased iWUE already reported for this species in a nearby locality (Granda et al. 2014), and are in agreement with predicted higher responsiveness of sclerophyllous species to CO_2 levels (Niinemets et al. 2011) and recent increase in climatic sensitivity in *J. thurifera* (Rozas and Olano 2013). However, the strong positive correlation between BAI and iWUE raw values was coupled to a significant negative correlation between their high-frequency inter-annual variations, as previously found for other drought-constrained conifers (Andreu et al. 2008; Eilmann et al. 2010). Standardized (annual variability) iWUE rates were negatively associated with carbon fixation levels, suggesting that enhanced iWUE caused a reduction in both leaf conductance and photosynthetic activity.

A positive long-term (decadal) correlation between iWUE and BAI, simultaneously with a negative short-term (yearly) correlation between the same variables, provides robust evidence that explains deviations from the projected CO_2-induced growth enhancement. Our results are consistent with a drought-induced limitation of tree growth response to rising CO_2, despite the trend of rising iWUE being maintained. Thus, even under a scenario of gradual CO_2 increase, increased iWUE may not compensate for the detrimental effect of more frequent and intense droughts (Linares and Camarero 2011; Heres et al. 2013; Perry et al. 2013).

This work reveals the complex set of interactions between climate, iWUE, secondary growth dynamics, and wood anatomical characteristics occurring under a drought-constrained Mediterranean environment. Water availability during the growing season significantly modulated tree growth at the xylem level, where all stages of xylogenesis were affected by June precipitation. Robust negative relationships of standardized yearly iWUE values with all carbon sinks (secondary growth, wall thickness, and amount of ray parenchyma), and the absence of significant relation between iWUE and lumen parameters, support the idea that an increase in water-use efficiency was simultaneous with a decline in carbon fixation in the xylem. Although our results support an effect of water availability and atmospheric CO_2 on secondary growth, it should be taken into account that carbon gain depends on multiple factors, including temperature, atmospheric vapor pressure deficit, and nutrient availability, among others. Furthermore, since iWUE is a ratio, the relationship between iWUE and BAI may be a consequence of changes in either photosynthetic rates, transpiration rates, or both. Thus, we cannot quantify which of both factors plays a more relevant role in determining secondary growth and xylem anatomy, since a reduction in secondary growth could respond to a proportional decline in carbon gain, but it also might be related to shifts in carbon allocation patterns.

Our results do not preclude the positive long-term effects of CO_2-induced iWUE increases on secondary growth, but remark the need to explore this relationship at different temporal scales to fully understand the actual links between iWUE and secondary growth dynamics.

Acknowledgments We are indebted to Ayuntamiento de Cabrejas del Pinar (Soria) for all the facilities provided during field work, Juan Carlos Rubio for assistance with stem disk preparation, and especially to Gonzalo Juste, Isabel Lorente, Maika Folch, and Enrique Marcos for the arduous task of microtomy, tracheid measurements, and isotope material preparation. David Brown edited the English. Comments and suggestions from Georg von Arx, David Tissue, and two anonymous reviewers greatly improved the paper. This work was supported by a FPI-EHU grant to A.A., a FPI-MICINN grant to A.I.G.-C. and projects CGL2012-34209 (Spanish Ministry of Economy and Competitivity) and VA006A10-2 (Junta de Castilla y León).

References

Andreu L, Planells O, Gutierrez E, Helle G, Schleser GH (2008) Climatic significance of tree-ring width and δ^{13} C in a Spanish pine forest network. Tellus B 60:771–781

Arbuckle JL (2009) Amos 18 user's guide. SPSS Inc, Chicago

Barber VA, Juday GP, Finney BP (2000) Reduced growth of Alaskan white spruce in the twentieth century from temperature-induced drought stress. Nature 405:668–673. doi:10.1038/35015049

Bert D, Leavitt SW, Dupouey J-L (1997) Variations of wood δ^{13}C and water-use efficiency of *Abies alba* during the last century. Ecology 78:1588–1596. doi:10.1890/0012-9658(1997)078[1588:VOWCAW]2.0.CO;2

Biondi F, Qeadan F (2008) A theory-driven approach to tree-ring standardization: defining the biological trend from expected basal area increment. Tree-Ring Res 64:81–96. doi:10.3959/2008-6.1

Camarero JJ, Olano JM, Parras A (2010) Plastic bimodal xylogenesis in conifers from continental Mediterranean climates. New Phytol 185:471–480. doi:10.1111/j.1469-8137.2009.03073.x

Chave J, Coomes D, Jansen S, Lewis SL, Swenson NG, Zanne AE (2009) Towards a worldwide wood economics spectrum. Ecol Lett 12:351–366. doi:10.1111/j.1461-0248.2009.01285.x

Cook ER, Holmes RL (1996) Guide for computer program ARSTAN. In: Grissino-Mayer HD, Holmes RL, Fritts HC (eds) The international tree ring data bank program library version 2.0 user's manual. Laboratory of Tree-Ring Research, University of Arizona, Tucson, pp 75–87

Cuny HE, Rathgeber CBK, Kiesse TS, Hartmann FP, Barbeito I, Fournier M (2013) Generalized additive models reveal the intrinsic complexity of wood formation dynamics. J Exp Bot 64:1983–1994. doi:10.1093/jxb/ert057

Dawes M, Hagedorn F, Handa I, Streit K, Ekblad A, Rixen C, Körner C, Hättenschwiler S (2013) An alpine treeline in a carbon dioxide-rich world: synthesis of a nine-year free-air carbon dioxide enrichment study. Oecologia 171:623–637. doi:10.1007/s00442-012-2576-5

Denne MP (1988) Definition of latewood according to Mork (1928). IAWA Bull 10:59–62

DeSoto L, de la Cruz M, Fonti P (2011) Intra-annual patterns of tracheid size in the Mediterranean tree *Juniperus thurifera* as an indicator for seasonal water stress. Can J For Res 41:1280–1294. doi:10.1139/X11-045

DeSoto L, Camarero JJ, Olano JM, Rozas V (2012) Geographically structured and temporally unstable growth responses of *Juniperus thurifera* to recent climate variability in the Iberian Peninsula. Eur J For Res 131:905–917. doi:10.1007/s10342-011-0564-7

Eilmann B, Buchmann N, Siegwolf R, Saurer M, Cherubini P, Rigling A (2010) Fast response of Scots pine to improved water availability reflected in tree-ring width and d13C. Plant Cell Environ 33:1351–1360. doi:10.1111/j.1365-3040.2010.02153.x

Eilmann B, Zweifel R, Buchmann N, Graf Pannatier E, Rigling A (2011) Drought alters timing, quantity, and quality of wood formation in Scots pine. J Exp Bot 62:2763–2771. doi:10.1093/jxb/erq443

Farquhar GD, Richards RA (1984) Isotopic composition of plant carbon correlates with water-use efficiency of wheat genotypes. Aust J Plant Physiol 11:539–552

Ferrio JP, Voltas J (2005) Carbon and oxygen isotope ratios in wood constituents of *Pinus halepensis* as indicators of precipitation, temperature and vapor pressure deficit. Tellus B 57:164–173. doi:10.1111/j.1600-0889.2005.00137.x

Fonti P, von Arx G, García-González I, Eilmann B, Sass-Klaassen U, Gärtner H, Eckstein D (2010) Studying global change through investigation of the plastic responses of xylem anatomy in tree rings. New Phytol 185:42–53. doi:10.1111/j.1469-8137.2009.03030.x

Galiano L, Martínez-Vilalta J, Lloret F (2011) Carbon reserves and canopy defoliation determine the recovery of Scots pine 4 yr. after a drought episode. New Phytol 190:750–759. doi:10.1111/j.1469-8137.2010.03628.x

Gimeno TE, Camarero JJ, Granda E, Pías B, Valladares F (2012) Enhanced growth of *Juniperus thurifera* under a warmer climate is explained by a positive carbon gain under cold and drought. Tree Physiol 32:326–336. doi:10.1093/treephys/tps011

Grace JB (2006) Structural equation modeling and natural systems. Cambridge University Press, Cambridge

Granda E, Camarero JJ, Jimeno TE, Martínez-Fernández J, Valladares F (2013) Intensity and timing of warming and drought differentially affect growth patterns of co-occurring Mediterranean tree species. Eur J For Res 132:469–480. doi:10.1007/s10342-013-0687-0

Granda E, Rossatto DR, Camarero JJ, Voltas J, Valladares F (2014) Growth and carbon isotopes of Mediterranean trees reveal contrasting responses to increased carbon dioxide and drought. Oecologia 174:307–317. doi:10.1007/s00442-013-2742-4

Grissino-Mayer HD (2001) Evaluating crossdating accuracy: a manual and tutorial for the computer program COFECHA. Tree-Ring Res 57:205–221

Hacke UG, Sperry JS (2001) Functional and ecological xylem anatomy. Perspect Plant Ecol Evol Syst 4:97–115. doi:10.1078/1433-8319-00017

Helama S, Lindholm M, Timonen M, Eronen M (2004) Detection of climate signal in dendrochronological data analysis: a comparison of tree-ring standardization methods. Theor Appl Climatol 79:239–254. doi:10.1007/s00704-004-0077-0

Helle G, Schleser GH (2004) Beyond CO_2-fixation by RuBisCO: an interpretation of $^{13}C/^{12}C$ variations in tree rings from novel intra-seasonal studies on broad-leaf trees. Plant Cell Environ 27:367–380. doi:10.1111/j.0016-8025.2003.01159.x

Heres AM, Voltas J, López BC, Martínez-Vilalta J (2013) Drought-induced mortality selectively affects Scots pine trees that show limited intrinsic water-use efficiency responsiveness to raising atmospheric CO_2. Func Plant Biol 41:244–256. doi:10.1071/FP13067

IPCC (2013) Climate change 2013. The physical science basis. Working group I contribution to the fifth assessment report of the intergovernmental panel on climate change technical summary. Cambridge University Press, Cambridge

Kilpeläinen A, Zubizarreta-Gerendiain A, Luostarinen K, Peltola H, Kellomäki S (2007) Elevated temperature and CO_2 concentration effects on xylem anatomy of Scots pine. Tree Physiol 27:1329–1338. doi:10.1093/treephys/27.9.1329

Koehler IH, Macdonald A, Schnyder H (2012) Nutrient supply enhanced the increase in intrinsic water-use efficiency of a temperate seminatural grassland in the last century. Global Change Biol 18:3367–3376. doi:10.1111/j.1365-2486.2012.02781.x

Körner C (2000) Biosphere responses to CO_2 enrichment. Ecol Appl 10:1590–1619. doi:10.1890/1051-0761(2000)010[1590:BRTCE]2.0.CO;2

Linares JC, Camarero JJ (2011) From pattern to process, linking intrinsic water-use efficiency to drought-induced forest decline. Global Change Biol 18:1000–1015. doi:10.1111/j.1365-2486.2011.02566.x

Linares JC, Delgado-Huertas A, Camarero JJ, Merino J, Carreira JA (2009) Competition and drought limit the response of water-use efficiency to rising atmospheric carbon dioxide in the Mediterranean fir *Abies pinsapo*. Oecologia 161:611–624. doi:10.1007/s00442-009-1409-7

Maseyk K, Hemming D, Angert A, Leavitt SW, Yakir D (2011) Increase in water-use efficiency and underlying processes in pine forests across a precipitation gradient in the dry Mediterranean region over the past 30 years. Oecologia 167:573–585. doi:10.1007/s00442-011-2010-4

McCarroll D, Loader NJ (2004) Stable isotopes in tree rings. Quat Sci Rev 23:771–801. doi:10.1016/j.quascirev.2003.06.017

McDowell NG (2011) Mechanisms linking drought, hydraulics, carbon metabolism, and vegetation mortality. Plant Physiol 155:1051–1059. doi:10.1104/pp.110.170704

Niinemets Ü, Flexas J, Peñuelas J (2011) Evergreens favored by higher responsiveness to increased CO_2. Trends Ecol Evol 26:136–142. doi:10.1016/j.tree.2010.12.012

Norby RJ, Warren JM, Iversen CM, Medlyn BE, McMurtrie RE (2010) CO_2 enhancement of forest productivity constrained by limited nitrogen availability. P Natl Acad Sci USA 107:19368–19373. doi:10.1073/pnas.1006463107

Offermann C, Ferrio JP, Holst J, Grote R, Siegwolf R, Kayler Z, Gessler A (2011) The long way down: are carbon and oxygen isotope signals in the tree ring uncoupled from canopy physiological processes? Tree Physiol 31:1088–1102. doi:10.1093/treephys/tpr093

Olano JM, Rozas V, Bartolomé D, Sanz D (2008) Effects of changes in traditional management on height and radial growth patterns in a *Juniperus thurifera* L. woodland. For Ecol Manage 255:506–512. doi:10.1016/j.foreco.2007.09.015

Olano JM, Eugenio M, García-Cervigón AI, Folch M, Rozas V (2012) Quantitative tracheid anatomy reveals a complex environmental control of wood structure in continental Mediterranean climate. Int J Plant Sci 173:137–149. doi:10.1086/663165

Olano JM, Almería I, Eugenio M, von Arx G (2013a) Under pressure, how a Mediterranean high-mountain forb coordinates growth and hydraulic xylem anatomy in response to temperature and water constraints. Funct Ecol 27:1295–1303. doi:10.1111/1365-2435.12144

Olano JM, Arzac A, García-Cervigón A, von Arx G, Rozas V (2013b) New star on the stage: amount of ray parenchyma in tree rings shows a link to climate. New Phytol 198:486–495. doi:10.1111/nph.12113

Pasho E, Camarero JJ, De Luis M, Vicente-Serrano SM (2011) Impacts of drought at different time scales on forest growth across a wide climatic gradient in north-eastern Spain. Agr For Meteorol 151:1800–1811. doi:10.1016/j.agrformet.2011.07.018

Peñuelas J, Canadell JG, Ogaya R (2011) Increased water-use efficiency during the 20th century did not translate into enhanced tree growth. Global Ecol Biogeogr 20:597–608. doi:10.1111/j.1466-8238.2010.00608.x

Perry LG, Shafroth PB, Blumenthal DM, Morgan JA, LeCain DR (2013) Elevated CO_2 does not offset greater water stress predicted under climate change for native and exotic riparian plants. New Phytol 197:532–543. doi:10.1111/nph.12030

Ponton S, Dupouey JL, Breda N, Feuillat F, Bodenes C, Dreyer E (2001) Carbon isotope discrimination and wood anatomy variations in mixed stands of *Quercus robur* and *Quercus petraea*. Plant Cell Environ 24:861–868. doi:10.1046/j.0016-8025.2001.00733.x

R Development Core Team (2011) R: a language and environment for statistical computing. R Foundation for Statistical Computing, Vienna

Rathgeber CBK, Rossi S, Bontemps JD (2011) Cambial activity related to tree size in a mature silver-fir plantation. Ann Bot 108:429–438. doi:10.1093/aob/mcr168

Roden JS, Farquhar GD (2012) A controlled test of the dual-isotope approach for the interpretation of stable carbon and oxygen isotope ratio variation in tree rings. Tree Physiol 32:490–503. doi:10.1093/treephys/tps019

Rozas V, Olano JM (2013) Environmental heterogeneity and neighbourhood interference modulate the individual response of *Juniperus thurifera* tree-ring growth to climate. Dendrochronologia 31:105–113. doi:10.1016/j.dendro.2012.09.001

Rozas V, DeSoto L, Olano JM (2009) Sex-specific, age-dependent sensitivity of tree-ring growth to climate in the dioecious tree *Juniperus thurifera*. New Phytol 182:687–697. doi:10.1111/j.1469-8137.2009.02770.x

Salleo S, Trifilo P, Esposito S, Nardini A, Lo Gullo MA (2009) Starch-to-sugar conversion in wood parenchyma of field-growing *Laurus nobilis* plants: a component of the signal pathway for embolism repair? Funct Plant Biol 36:815–825. doi:10.1071/FP09103

Saurer M, Siegwolf R, Schweingruber F (2004) Carbon isotope discrimination indicates improving water-use efficiency of trees in northern Eurasia over the last 100 years. Global Change Biol 10:2109–2120. doi:10.1111/j.1365-2486.2004.00869.x

Speed JDM, Austrheim G, Hester AJ, Mysterud A (2011) Browsing interacts with climate to determine tree-ring increment. Funct Ecol 25:1018–1023. doi:10.1111/j.1365-2435.2011.01877.x

Taylor AM, Brooks JR, Lachenbruch B, Morrell JJ, Voelker S (2008) Correlation of carbon isotope ratios in the cellulose and wood extractives of Douglas-fir. Dendrochronologia 26:125–131. doi:10.1016/j.dendro.2007.05.005

Tyree MT (2003) Hydraulic limits on tree performance: transpiration, carbon gain and growth of trees. Trees 17:95–100. doi:10.1007/s00468-002-0227-x

Vicente-Serrano SM, Beguería S, López-Moreno JI (2010) A multiscalar drought index sensitive to global warming: the standardized precipitation evapotranspiration index (SPEI). J Climate 23:1696–1718. doi:10.1029/2003WR002610

Von Wilpert K (1991) Intra-annual variation of radial tracheid diameters as a monitor of site specific water stress. Dendrochronologia 9:95–114

Waterhouse JS, Switsur VR, Barker AC, Carter AHC, Hemming DL, Loader NJ, Robertson I (2004) Northern European trees show a progressively diminishing response to increasing atmospheric carbon dioxide concentrations. Quat Sci Rev 23:803–810. doi:10.1016/j.quascirev.2003.06.011

Ze-Xin F, Shi-Bao Z, Guang-You H, Slik JWF, Cao K-F (2012) Hydraulic conductivity traits predict growth rates and adult stature of 40 Asian tropical tree species better than wood density. J Ecol 100:732–741. doi:10.1111/j.1365-2745.2011.01939.x